

Automated detection of fecal contamination of apples based on multispectral fluorescence image fusion [☆]

Moon S. Kim ^{a,*}, Alan M. Lefcourt ^a, Yud-Ren Chen ^a, Yang Tao ^b

^a *United States Department of Agriculture, Instrumentation and Sensing Laboratory, Henry A. Wallace Beltsville Agricultural Research Center, Bldg 303 BARC-East, 10300 Baltimore Ave, Power Mill Rd., Beltsville, MD 20705-2350, United States*

^b *Bioimaging and Machine Vision Laboratory, University of Maryland, College Park, MD 20742, United States*

Received 4 March 2004; received in revised form 15 September 2004; accepted 22 October 2004

Available online 8 December 2004

Abstract

Fluorescence techniques have shown great potential for detecting animal feces on foods. A recently developed field portable multispectral fluorescence imaging system was used to acquire steady-state fluorescence images of feces contaminated apples. Twenty Red Delicious apples encompassing natural color variation were artificially contaminated with dairy cow feces to create five fecal contamination spots on each apple. The feces spots were not clearly visible to the human eye. Multispectral fluorescence images, with wavebands centered at the red emission peaks of cow feces and apples, in addition to blue and green bands, were evaluated to determine an optimal red band for detection of feces contamination spots on apples. The results show that fluorescence emission bands at 670 nm provided the greatest potential for the detection of feces contamination on apples. In addition, investigation of multispectral fusion methods indicated that band ratio image of 670 nm to 450 nm or 550 nm improve sensitivity of detection. Two-band ratios along with the use of unsupervised histogram-based thresholding allowed detection of cow feces contaminations on apples regardless of apple colorations with a 100% success rate.

© 2004 Elsevier Ltd. All rights reserved.

Keywords: Fluorescence imaging; Multispectral; Food safety; Fecal contamination; Apples

1. Introduction

An alarming number of people are affected by food-borne illness each year; thus safe production of food commodities is an issue of public concern (Armstrong, Hollingsworth, & Morris, 1996; Mead et al., 1999). Animal fecal matter is the primary source of pathogenic bacteria on meat products and in unpasteurized apple juice (Cody et al., 1999). Current government regulations stipulate no-visual evidence of fecal matter on

meats or on fruits used to make juices (FDA, 2001; FSIS, USDA, 1998). Researchers at the Instrumentation and Sensing Laboratory (ISL), Agricultural Research Services (ARS), United States Department of Agriculture (USDA) in Beltsville, MD have been working to develop new methodologies to provide a rapid, nondestructive means to detect fecal contamination of fruits and vegetables.

Approaches for nondestructive detection for food quality and safety inspections typically utilize spectroscopic or optical sensing techniques including machine vision and multispectral imaging (Chen, Chao, & Kim, 2002; Chen, Huffman, Park, & Nguyen, 1996; Park, Chen, & Nguyen, 1998). Due to the potentially increased sensitivity, fluorescence techniques have great potential in food quality and safety inspections (Kim,

[☆] Company and product names are used for clarity and do not imply any endorsement by USDA to the exclusion of other comparable products.

* Tel.: +1 301 504 8450; fax: +1 301 504 9466.

E-mail address: kimm@ba.ars.usda.gov (M.S. Kim).

Chen, & Mehl, 2001a). The advent of new sensor technologies and peripherals make the on-line use of fluorescence techniques feasible. We have developed several fluorescence imaging systems capable of rapidly capturing multispectral images even in the presence of ambient light (Kim, Lefcourt, & Chen, 2003a; Lefcourt, Kim, & Chen, 2003).

Animal feces from cow, deer, and swine exhibit strong fluorescence emissions in the red region of the spectrum (Kim, Lefcourt, & Chen, 2003b). The red fluorescence emissions with peaks at near 675 nm emanate from chlorophyll *a* or its metabolites such as pheophorbide *a* originating from green roughages consumed by the animals. The emission peak from the animal feces is blue-shifted when compared to the chlorophyll *a* emission peak typically observed in intact apples at 685 nm.

Based on the fluorescence emission characteristics of cow feces and apples, four band-pass filters in the red region with different center wavelengths and bandwidths, and one each in the blue and green regions, were analyzed to determine optimal red band for detection of fecal contamination on apples. Apples were artificially contaminated with fresh dairy cow feces to create contamination spots that were not clearly visible to the human eyes. A combination of simple two-band ratios as a multispectral fusion method in conjunction with the use of unsupervised, histogram-based, automated threshold classification was evaluated for detection of feces contamination spots on apples. A recently developed portable fluorescence imaging system was used to acquire images of apples with feces contamination spots at six spectral bands.

2. Materials and methods

2.1. Samples and feces application

Apples, cultivar 'Red Delicious', were "tree run" (no coating of wax or fungicide) and were acquired from Rice Fruit Company (Gardner, PA) during the 2002 harvest season. The samples were transported to the ISL laboratory, and stored in a cold room (3 °C). Individual apples display color variations that result from differential growth conditions (i.e., solar exposure) which in turn, cause differences in pigmentation concentrations and ripeness. For instance, sun-exposed sides ripen faster than sides given less exposure to direct solar radiation. Color variations generally range from near-uniform red to variegated red and green colors on sun-exposed and shaded sides, respectively.

Fresh cow feces from animals fed feedstuffs containing green roughage were collected from USDA farm facilities in Beltsville, MD using 50 ml polypropylene vials and stored at 4 °C prior to use. With self-adhesive labels (Avery Dennison Office Supply, Diamond Bar,

CA), 20 stencils each with five, 5 mm diameter, circular holes in an "X" pattern were created using a cork-borer. The stencils were applied on the sides of 20 Red Delicious apples to include a range of the natural skin colorations without physical defects. An approximately 3 mm thick layer of fresh feces was applied on the stencils to cover individual holes and was let to dry overnight at room temperature (20 °C). The stencils were removed from the apples the next day, which also removed the patches of dry feces leaving minimal feces residue on the apple surfaces. The resultant fecal contamination spots were not readily visible to the human eye. It was found that one of the apples was other than Red Delicious; this apple was replaced a day later with a Red Delicious apple. Note that a preliminary test was performed on several apples to ensure that the use of self-adhesive stencils did not create any artifacts on the apples surfaces that were detectable by the fluorescence imaging system.

2.2. Transportable multispectral steady-state fluorescence imaging system

A schematic diagram of the transportable multispectral fluorescence imaging system (TMFIS) is shown in Fig. 1. The imaging device consists of an intensified-

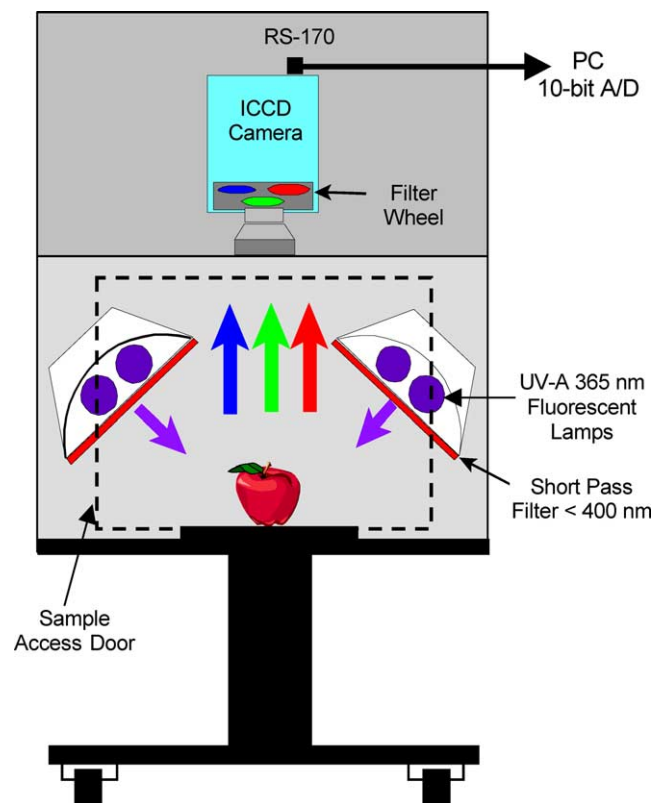


Fig. 1. Schematic diagram of the transportable multispectral steady-state fluorescence imaging system.

CCD (ICCD) camera (IMC-201, Xybion Electronics Systems, CA) equipped with an integrated filter wheel that can accommodate up to six, 25 mm interference filters. The ICCD camera is coupled to a f 1.4 c-mount lens (Rainbow optics, CA, USA). The image resolution was set at 480 (H) × 640 (V) pixels, and the signal outputted as RS-170. Images are digitized using a 10-bit A/D frame-grabber with a 30 Hz refresh rate (PCI-1409, National Instruments). Note that the 10-bit A/D was used to obtain greater dynamic response range (and to improve the signal to noise ratio) of the fluorescence emission compared to 8-bit devices typically used for video.

Four ultraviolet (UV-A: 320–400 nm) fluorescent lamp assemblies (Model EA-180/12, Spectronics Corp., NY) are used as the excitation source. Each lamp assembly is mounted on sides of a 44 × 44 cm rectangular frame, and is tilted 45° toward the center of the FOV. This arrangement provides a near uniform target illumination. A 5 × 15 cm short-pass (<400 nm) filter (UG1, Schott Glass Co. PA) is mounted in front of each UV lamp assembly. This prevents potential for detecting scattered excitation light greater than 400 nm as fluorescence emission from samples materials.

The imaging sensor and lighting peripherals are enclosed in a light-tight, transportable container (60 × 60 × 75 cm) equipped with a front access door panel for sample placement. Light-tight air intake and exhaust outlet with an electrical fan circulate air to maintain the container at room temperature.

2.3. Multispectral band selection

The ICCD camera allows imaging up to six independent spectral bands. Selection of wavelengths and bandwidths of the filters were based on the emission characteristics of apples and cow feces; note that selection of filter parameters were limited by commercial availability. When excited with UV-A radiation, a number of compounds found in plants emit fluorescence in the visible region with emission peaks occurring approximately at 450 and 685 nm (Chappelle, McMurtrey, & Kim, 1991; Lang, Stober, & Lichtenthaler, 1991). In addition, an emission shoulder at 530 nm and a secondary peak in the 720–730 nm are observed. Fluorescence emissions in the blue–green regions are broad in nature, and blue and green interference filters centered at 450 nm (F450) and 550 nm (F550), respectively, each with 40 nm FWHM (Full Width at Half Maximum), were chosen.

Of particular interest for detection of animal fecal contamination is fluorescence emission in the red region of the spectrum. Red fluorescence emission peak of cow feces is blue-shifted (approximately 10 nm) compared to chlorophyll *a* emission peak typically observed from intact plant materials at 685 nm. Thus, narrow filters

(10 nm FWHM) centered at 670 (F670) and 685 nm (F685) were selected. For the remaining two filter positions, 678 nm (F680) filter with 22 nm FWHM encompassing both red emission peaks and 700 nm (F700) filter with 40 nm FWHM spanning the F685 and secondary emission peak region (chlorophyll *a* spillover) were chosen.

2.4. Image acquisition

PC Interface software (MS Windows, Visual Basic, Version 6.0) was developed to control the imaging system and acquired image data. Filter position and corresponding ICCD parameters, gain (0–100%) and exposure time (0–33.333 ms), were controlled via RS-232. Independent intensifier gain and CCD exposure time set for each filter position were determined to utilize approximately the half of the dynamic range of the system for typical sample materials in the study. Six individual band images per apple were sequentially captured and stored in a 16-bit signed integer, binary file for later analyses along with a header file containing imaging parameters. The automated acquisitions of six images required approximately 50 s. Dark current and flat-field correction files were also acquired to correct images for heterogeneous responses of the system due to lighting and optics. Readers are referred to an article by Kim et al. (2001b) for flat-field correction procedures.

2.5. Image analyses

A histogram-based, simple threshold method was used to create binary-classification images of feces contaminated spots on apples. In order to determine threshold values without human-bias, a nonparametric and unsupervised automated histogram threshold method described by Otsu (1979) was modified and used for this study. It was originally developed to determine a threshold value based on histogram of 8-bit gray scale. We modified it to work with 16-bit images. Individual bands and ratios of red bands to blue and green images were subjected to the modified Otsu method. For two-band ratio images, the ratio values were linearly transformed to span 16-bit scale. In order to allow analyses of only the apple surface area, masking operations were performed on individual bands using apple surface-mask image generated by applying the automated thresholding to green band images.

We developed PC-based image processing/analyses software in MS Windows, Visual Basic to perform following functions: dark current subtraction and flat-field corrections, image visualization/enhancement, multiple image merging, background masking, pixel binning, simple and automated (i.e., modified Otsu) thresholdings, and arithmetic operations (i.e., band ratio). The

software included tools to determine the descriptive statistics of a rectangular region of interest (ROI). Images presented in the figure are linearly transformed (1% minimum and maximum histogram thresholding) gray scale in standard 8-bit bitmap format.

3. Results and discussion

Fig. 2 illustrates fluorescence images at F450, F550, F670, F680, F685, and F700 of representative apples with five feces contaminated spots acquired using the TMFIS. Natural intensity variations between apples are apparent in that the shaded sides (upper two apples) exhibit relative higher fluorescence intensities compared to the sun-exposed apples throughout the spectral bands under investigation. In the blue band (F450), only the shaded apples show the evidence of the feces contamination regions as slightly darker spots compared to the surrounding apple surfaces. The white spots seen in the blue band are due to particulate matters that typically emit relatively high fluorescence. The green band (F550) shows the lenticles as white dots on apples. For the sun-exposed apples with uniform dark-reddish color, no evidence of feces contamination is observed in the blue–green region of the spectrum.

In the red band images (Fig. 2c–f), feces contaminated regions are discernable as white spots (with varying degrees among the four bands) in the sun-exposed and some of the shaded apples. In general, the fluorescence responses of the feces contamination spots appear to be additive (transparent feces and underlying apple

surfaces) in that feces spots on the shaded apple surfaces are brighter compared to the sun-exposed sides. As shown in the upper-left apple images at F680, F685, and F700 (Fig. 2d–f, respectively), the fluorescence emissions from the shaded apple surfaces (with highly variegated greenish coloration) are as high as the feces spots. However at F670, the feces contamination spots show relatively higher fluorescence intensities compared to the surrounding apple surfaces. F670 band image also exhibits smaller fluorescence variations within individual apples compared to other red bands, especially for the greenish apples. This observation suggests that the F670 band, where cow feces exhibits emission peak and a shorter wavelength than the chlorophyll *a* peak from apples, may be the optimal red spectral region for detection of animal fecal matter in the presence of chlorophyll *a* fluorescence emission in the background.

When apples are analyzed individual band basis for detection of fecal contamination spots, fluorescence intensity variations of the apples and the additive nature of fluorescence responses from the feces and apples hinder the use of a simplified-detection method (i.e., simple threshold). For instance, F670 band shows relatively higher fluorescence from feces compared to the apples regardless of the apple colorations. However, simple threshold values for discriminating the feces contamination on the shaded sides are different from the sun-exposed side apples (resultant figure omitted for brevity). Furthermore, natural feces contamination on apples occurs without known size and shape. The lack of the morphological information along with the dynamic fluorescence responses of the samples add to the

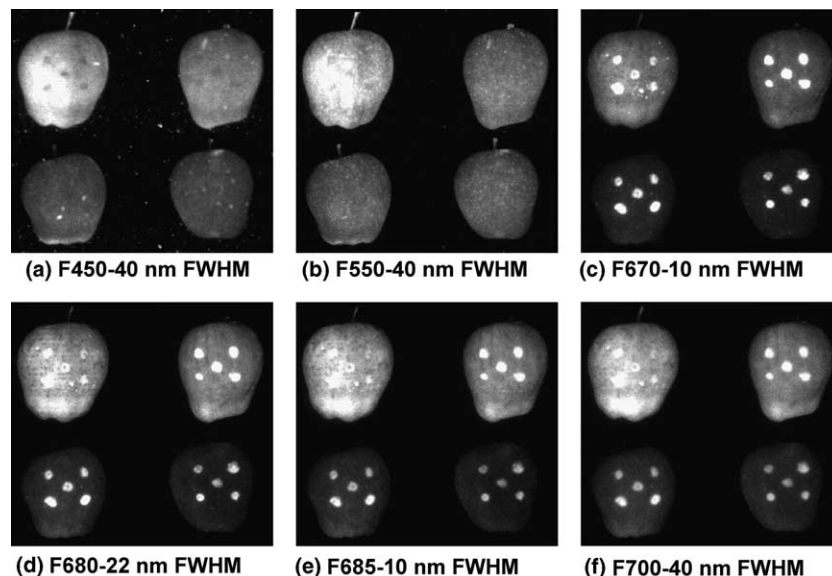


Fig. 2. Steady-state fluorescence images of the shaded (top two apples) and sun-exposed (bottom two) sides of apples with five cow feces contamination spots acquired by the transportable multispectral fluorescence imaging system at F450, F550, F670, F680, F685, and F700. Note that images of individual apples were acquired separately and a composite of four apples, shaded and sun-exposed sides, were created to show the effects of apple color variations in fluorescence responses.

complexities in recognition of the feces contaminated spots on apples using a single fluorescence band.

Normalization of the dynamic fluorescence responses due to the effects of apple colorations may be needed to allow the use of a simplified-detection regime. The goal of using multispectral approach in this investigation is to find a use of more than a single spectral domain to minimize the fluorescence variations of apples with various colorations. A ratio of red band to either blue or green fluorescence band may potentially normalize the effects of apple colorations and enhanced the contrast between the feces contaminated spots and apple surfaces (Kim et al., 2002). In order to examine the proposed method under the various apple colorations, images of the 20 individual apples were combined to create one large image at each band, ratio images were created and the automated threshold-analyses were performed to determine effective two-band ratio combinations for detection of feces contamination spots on apples regardless of the colorations.

Fig. 3a and b illustrate ratio images of sample shown in Fig. 2, two-band ratio combination of the red bands (F670, F680, F685, and F740) to F450 and F550 bands, respectively. Note that although only four representative apples are shown in the figure, discussions from this point on are generally based on the results observed in all 20 samples. For the sun-exposed sides apples, all the ratio images exhibit clear outlines of the feces contamination spots. However, the ratio results from the shaded side apples show differential responses when compared to the results for the sun-exposed side apples, except for F670/F450 and F670/F550. The figure sug-

gests that F670 to F450 and F550 ratios yield minimal variations in apple surfaces regardless of the colorations and clear outlines of the feces contamination spots. These observations are further evident when histograms for the ratio images are examined.

Fig. 4a–d illustrates histograms for ratio images of F670/F450, F670/F550, F680/F450, and F680/F550. The histograms manifest that these two-band ratios result near normal distributions for apple surfaces; the best ratio in terms of minimizing the variations due to apple colorations being F670/F450 ratio as suggested by the highest frequency and narrow width in pixel distributions (Fig. 4a). Histograms for the other ratio images, as suggested in Fig. 3, failed to show normalization of the apple surface variations and are omitted for brevity.

The use of modified Otsu method allowed the evaluation of ratio (and individual) images in terms of effectiveness for detection of feces contamination spots without human intervention. It also provided threshold values for automated classification of feces contamination spots on apples. The threshold values were determined to be 1.06, 1.20, 2.16, and 1.68 for F670/F450, F670/F550, F680/F450, and F680/F550 ratio images, respectively (also shown in Fig. 4).

Binary-classification images (detection results) created using the respective threshold values for F670/F450, F670/F550, and F680/F450 are shown in Fig. 5. In general, number of pixels classified as feces contamination spots were less for shaded side apples. The percent feces cover per apple were determined to span 2.38–7.93% (or 2280–6036 pixels). Overall, F670/F450,

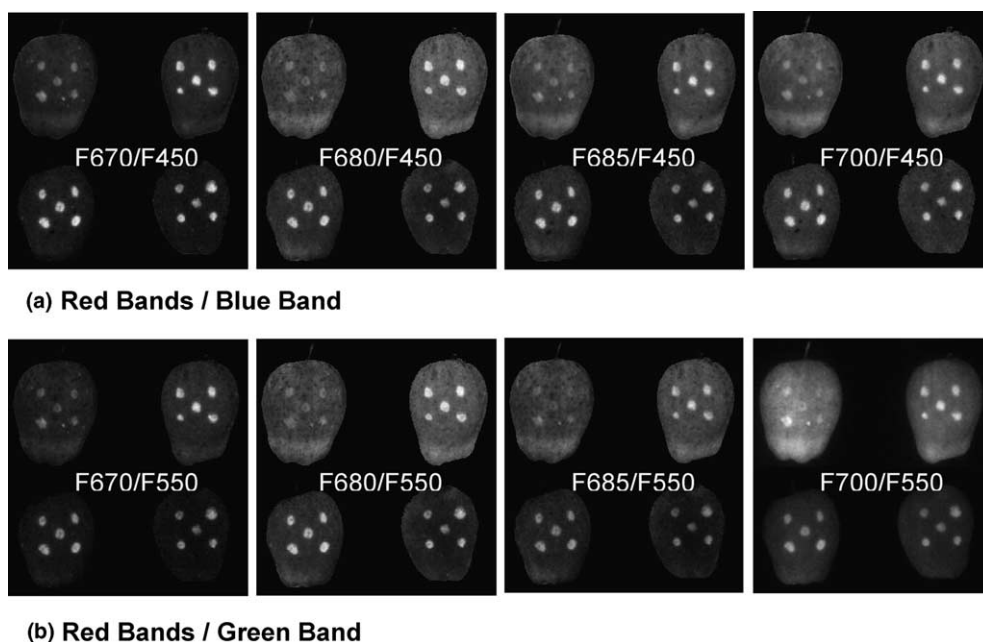


Fig. 3. Fluorescence ratio images of the red bands to blue band (a) and red bands to green band (b).

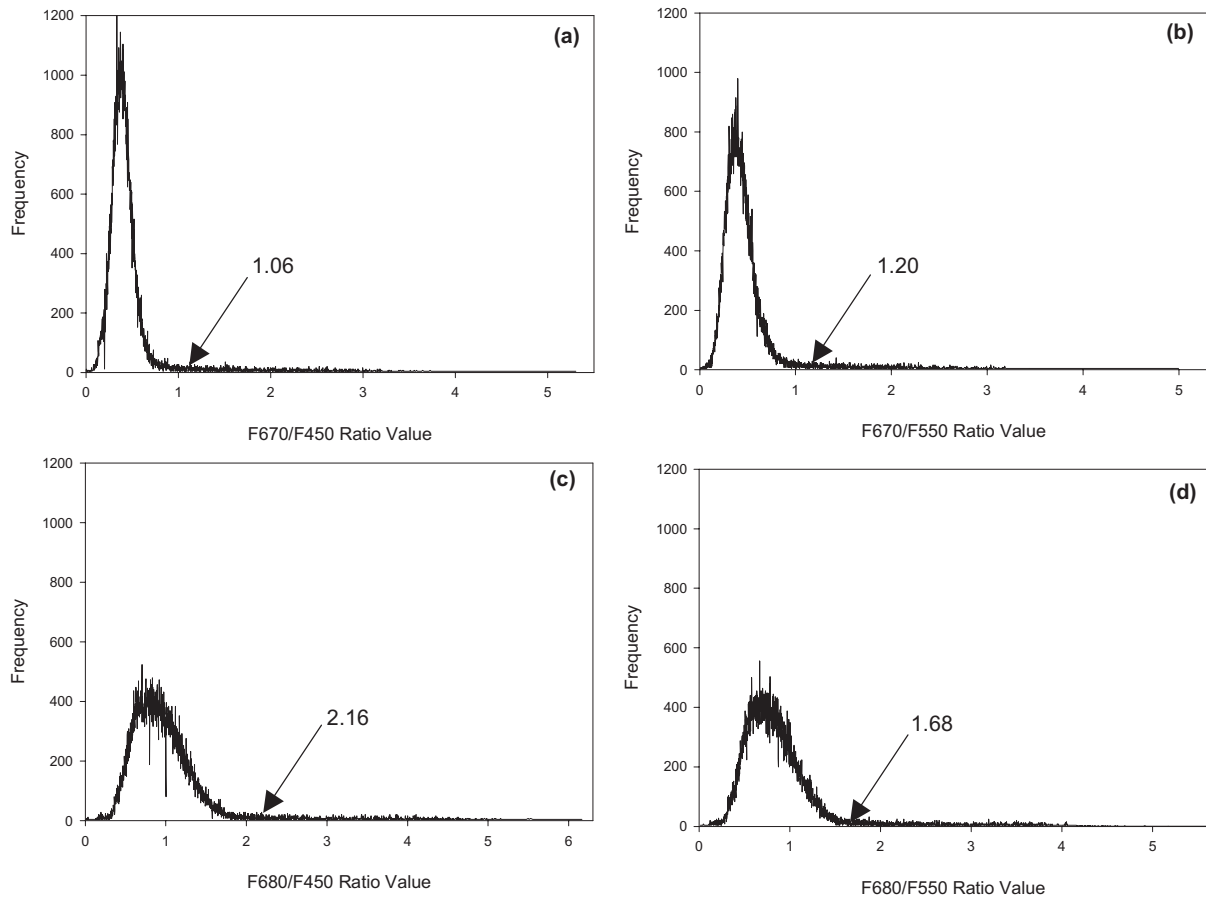


Fig. 4. Histograms for F670/F450 (a), F670/F550 (b), F680/F450 (c), and F680/F550 (d) ratio images. The ratio value scale (X -axis) spans the minimum and maximum ratio values. Note that histograms are those of ratio images containing all 20 apples under investigation. Also, threshold values determined by the modified Otsu method for the classification of the feces contamination spots on apples are indicated in the figure.

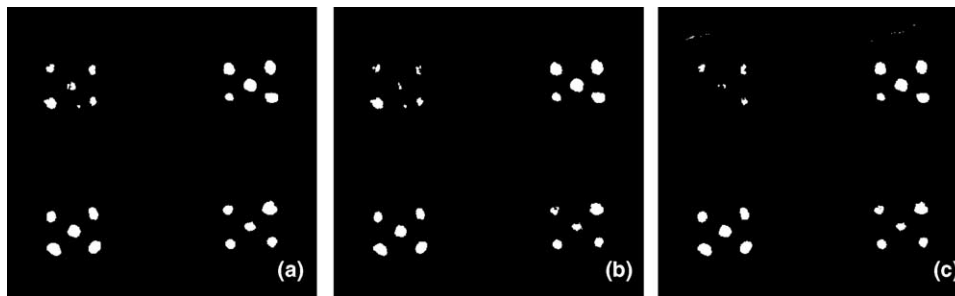


Fig. 5. Binary images (classification for feces contamination spots) for F670/F450 (a), F670/F550 (b), and F680/F450 (c) ratio images.

F670/F550, and F680/F450 ratios detected 100, 98, 97 out of 100 feces contamination spots on 20 apples, respectively. The resultant binary-classification images for the other ratios (figure not shown) contain significant portions of apple surfaces (false positives). As illustrated in Fig. 5c, F680/F450 detected increased levels of false positive (apple edge region) compared to F670/F450 and F670/F550. F670/F450 follow by F670/F550 were determined to be the best ratio images (e.g., 100% and 98% detection rates). This further suggests F670 as the

optimal red spectral band for detection of fecal contamination on apples.

However, for these two ratios, a small number of pixels numbering up to 50 and one or more clusters were observed on 5 out of 20 apples (examples shown on the upper-left shaded side apples in Fig. 5a and b). These small false positive spots may be actual feces contaminations that can arise during the sample preparation due to splatters and seepage through the paper stencils. It is also possible that some of these small spots may

emanate from natural fecal contamination; further investigation is needed to confirm this possibility. Various spatial filters are readily available that can exclude small spots (false positives) from being detected as feces contamination spots (Lefcourt et al., 2003).

4. Conclusions

In this study, with the use of a recently developed multispectral fluorescence imaging system, we determined that 670 nm is the optimal red fluorescence waveband for detection of animal feces contamination on apples. Furthermore, by using a simple multispectral fusion method in conjunction with the use of unsupervised automated threshold algorithm, we demonstrated that 100% of the spots on apples artificially contaminated with dairy cow feces could be detected. The results shown in this investigation are further manifestation that fluorescence techniques are very sensitive optical tool and indicate that fluorescence-base systems can be used to detect fecal contamination that is not readily visible to the naked eye.

References

- Armstrong, G. L., Hollingsworth, J., & Morris, J. G. Jr., (1996). Emerging foodborne pathogens: *Escherichia coli* O157:H7 as a model of entry of a new pathogen into the food supply of the developed world. *Epidemiology Review*, 18, 29–51.
- Chappelle, E. W., McMurtrey, J. E., & Kim, M. S. (1991). Identification of the pigment responsible for the blue fluorescence band in laser induced fluorescence (LIF) spectra of green plants, and the potential use of this band in remotely estimating rates of photosynthesis. *Remote Sensing of Environment*, 36, 213–218.
- Chen, Y. R., Chao, K., & Kim, M. S. (2002). Future trends of machine vision technology for agricultural applications. *Computer Electronic in Agriculture*, 36, 173–191.
- Chen, Y. R., Huffman, R. W., Park, B., & Nguyen, M. (1996). Transportable spectrophotometer system for on-line classification of poultry carcasses. *Applied Spectroscopy*, 50(7), 910–916.
- Cody, S. H., Glynn, M. K., Farrar, J. A., Cairns, K. L., Griffin, P. M., Kobayashi, J., et al. (1999). An outbreak of *Escherichia coli* O157:H7 infection from unpasteurized commercial apple juice. *Annals of Internal Medicine*, 130, 202–209.
- FDA (2001). Hazard analysis and critical control point (HAACP); procedures for the safe and sanitary processing and importing of juices. *Federal Registry*, 66(13), 6137–6202.
- Food Safety Inspection Service (FSIS, USDA) (1998). Livestock post-mortem inspection activities-enforcing the zero tolerances for fecal materials, ingesta, and milk FSIS Directive 6420.1 (pp. 1–9) http://www/fsis.usda.gov/OPPDE/rdad/FSISDirectives/FSISDir6420_1.htm.
- Kim, M. S., Chen, Y. R., & Mehl, P. M. (2001a). Hyperspectral reflectance and fluorescence imaging system for food quality and safety. *Transaction of the ASAE*, 44(3), 721–729.
- Kim, M. S., Lefcourt, A. M., & Chen, Y. R. (2003a). Multispectral laser-induced fluorescence imaging system for large biological samples. *Applied Optics*, 42(19), 2934–3927.
- Kim, M. S., Lefcourt, A. M., & Chen, Y. R. (2003b). Optimal fluorescence excitation and emission bands for detection of fecal contamination. *Journal of Food Protection*, 66(7), 1198–1207.
- Kim, M. S., Lefcourt, A. M., Chen, Y. R., Kim, I., Chao, K., & Chan, D. (2002). Multispectral detection of fecal contamination on apples based on hyperspectral imagery—part II: Application of fluorescence imaging. *Transaction of the ASAE*, 45(6), 2039–2047.
- Kim, M. S., McMurtrey, J. E., Mulchi, C. L., Daughtry, C. S. T., Chappelle, E. W., & Chen, Y. R. (2001b). Steady-state multispectral fluorescence imaging system for plant leaves. *Applied Optics*, 40, 157–166.
- Lang, M., Stober, F., & Lichtenthaler, H. K. (1991). Fluorescence emission spectra of plant leaves and plant constituents. *Radiant Environment Biophysics*, 30, 333–347.
- Lefcourt, A. M., Kim, M. S., & Chen, Y. R. (2003). Automated detection of fecal contamination of apples by multispectral laser-induced fluorescence imaging. *Applied Optics*, 42(19), 3935–3943.
- Mead, P. S., Slutsker, L., Dietz, V., McCaig, L. F., Bresee, J. S., Shapiro, C., et al. (1999). Food-related illness and death in the United States. *Emerging Infectious Diseases*, 5, 607–625.
- Otsu, N. (1979). A threshold selection method from gray-level histograms. *IEEE Transactions on Systems, Man, and Cybernetics*, SMC, 9(1), 62–66.
- Park, B., Chen, Y. R., & Nguyen, M. (1998). Multi-spectral image analysis using neural network algorithm for inspection of poultry carcasses. *Journal of Agricultural Engineering Research*, 69(4), 351–363.